JOURNAL OF GEOPHYSICAL RESEARCH, VOL. 92, NO. A13, PAGES 15,225–15,233, DECEMBER 30, 1987

Electrostatic Waves in the Magnetosphere of Uranus

W. S. KURTH,[1] D. D. BARBOSA,[2] D. A. GURNETT,[1] AND F. L. SCARF[3]

During its encounter with Uranus the plasma wave receiver on Voyager 2 observed electrostatic waves similar in many respects to those observed in other planetary magnetospheres. The most prominent type observed was the Bernstein mode emissions between harmonics of the electron cyclotron frequency. As is the case at other planets, the most intense Bernstein waves were observed near the magnetic equator of the planet, even though the tilt of the Uranian magnetic moment with respect to the rotational axis is very large. A small offset in the location of these electrostatic waves from the equator predicted by the offset, tilted dipole magnetic field model suggests some warping of the magnetic equator due to ring currents or external currents flowing on the magnetopause. Other examples of electrostatic Bernstein waves were observed closer to the planet and at higher magnetic latitudes. The energy of resonant electrons is calculated to be a few hundred electron volts, and measurements of electrons with this energy indicate the critical flux required to drive the Bernstein mode is available. The existence of the Bernstein modes near the upper hybrid resonance frequency leads to estimates of the electron density at several locations within the Uranian magnetosphere, and these compare well with densities measured by the plasma science investigation. In addition to the Bernstein modes, a number of highly sporadic emissions were observed in the vicinity of the Miranda L shell. While the absolute determination of the mode of these waves is uncertain, it is likely that some are electrostatic modes. Since this region of the Uranian magnetosphere is very perturbed and interesting, we shall attempt to identify possible modes associated with the waves.

1. INTRODUCTION

The Voyager 2 encounter of Uranus in January 1986 provided the opportunity to observe yet another planetary magnetosphere and compare the plasma physical processes taking place there to those occurring in the magnetospheres of Earth, Jupiter, and Saturn. In particular, in this paper we survey electrostatic emissions observed at Uranus and apply our knowledge of similar emissions at Earth to establish similarities and differences in the signatures. In this way we can begin to understand how variations in the configuration of the Uranian magnetosphere might effect changes in the emissions. We can also use the known behavior of the electrostatic waves as diagnostic tools to lend insight into such questions as the variation of electron density within the magnetosphere and possibly some information about the configuration of the magnetic field itself.

Voyager 2 carried a plasma wave receiver designed to measure the amplitude of the electric fields associated with waves in the frequency range of 10 Hz to 56 kHz [*Scarf and Gurnett*, 1977]. The instrument utilizes a single electric dipole antenna for a sensor. Since no wave magnetic field measurements were made, information concerning the mode of propagation of the detected waves must be deduced from the spectral and temporal characteristics of the emissions, the relationship of the frequency of the emission to characteristic frequencies of the plasma, and comparisons with similar emissions studied at the Earth. Fortunately, most of the waves observed in the magnetospheres of the outer planets thus far are easily associated with terrestrial analogs; hence much progress can be made even without more sophisticated instrumentation and additional sensors.

An initial overview of plasma waves observed in the Uranian magnetosphere was given by *Gurnett et al.* [1986], and a general comparison with plasma waves observed at Jupiter and Saturn is included in this issue [*Scarf et al.*, this issue]. In this paper we shall detail the observations of electrostatic waves in the magnetosphere of Uranus, focusing primarily on the Bernstein or $(n + \frac{1}{2})f_c$ emissions where f_c is the electron cyclotron frequency $f_c[\text{Hz}] = 28|B|[\text{nT}]$. Bernstein waves were first observed at Earth by *Kennel et al.* [1970] and have been studied extensively both experimentally and theoretically by a large number of investigators (see, for example, *Christiansen et al.* [1978], *Ashour-Abdalla and Kennel* [1978], and *Kennel and Ashour-Abdalla* [1982] and references therein). Surveys of electrostatic waves at Jupiter and Saturn were given by *Barbosa and Kurth* [1980] and *Kurth et al.* [1980, 1983].

In section 2 we will present the observations of electrostatic waves, describing their location, bandwidths, frequencies, and intensities and giving provisional mode identifications, as possible. In section 3 we shall discuss the various implications of the electrostatic waves, including estimates of the electron density based on the frequency of the upper hybrid resonance band and a comment on the possible distortion of the distant magnetic equator identified by an offset in the location of Bernstein waves with respect to the magnetic equator given by the offset, tilted dipole (OTD) magnetic field model [*Ness et al.*, 1986]. Finally, a summary will be given in section 4.

2. OBSERVATIONS

Figure 1 provides a summary of the plasma wave spectrum observed by Voyager 2 as it traversed the magnetosphere of Uranus on January 24, 1986. For each of the 16 spectrum analyzer channels of the plasma wave receiver, Figure 1 includes an amplitude versus time representation in which the height of the solid region corresponds to the electric field strength averaged over 48 s. Where discernible, the line above the solid region corresponds to the peak electric field detected during each 48-s averaging interval. Using the baseline of each channel as a logarithmic frequency scale, the electron cyclotron frequency has been superimposed as a solid line based on measurements of the magnitude of the magnetic field provided

[1] Department of Physics and Astronomy, University of Iowa, Iowa City.
[2] Institute of Geophysics and Planetary Physics, University of California, Los Angeles.
[3] TRW Space and Technology Group, Redondo Beach, California.

Paper number 7A8921.
0148-0227/87/007A-8921$05.00

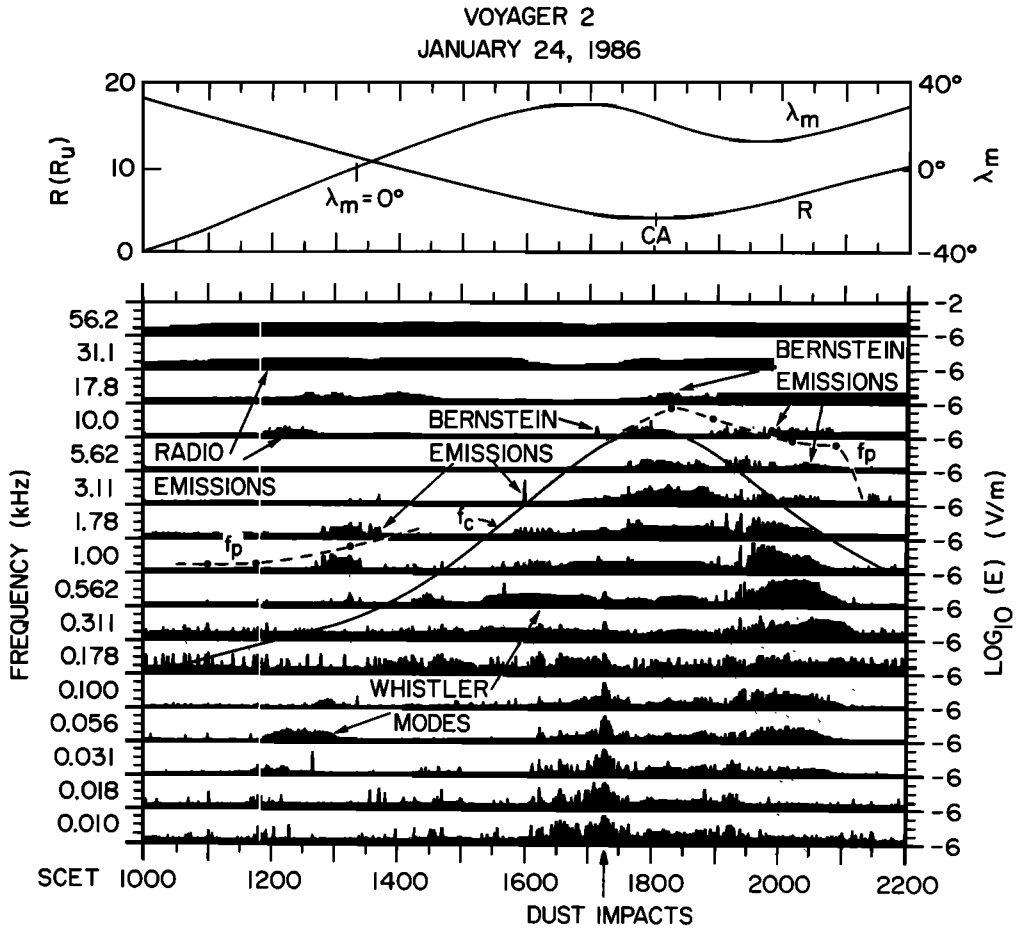

Fig. 1. Top: A plot of the Voyager radial distance R from Uranus and magnetic latitude λ_m based on the OTD field model [*Ness et al.*, 1986] as a function of time. Bottom: A summary of the Voyager 2 plasma wave observations in the magnetosphere of Uranus. The wave activity below the f_c contour (solid line) is primarily whistler mode radiation. The highest-frequency emissions are radio waves. The sporadic emissions just above the f_c contour are electrostatic Bernstein waves, generally extending up to about f_{UHR}. The bursty emissions near 1920 SCET below f_c are unidentified at this time, but it is possible that those below a few hundred hertz are Doppler-shifted ion acoustic waves. The dashed lines represent an electron plasma frequency profile based on our interpretation of the plasma and radio wave spectrum (see section 3.1). The bursty signature throughout the interval most apparent at 178 Hz but weakly visible at 311 Hz is thought to be interference, but the source is uncertain. The same signature is present even when the spacecraft is deep in the solar wind, far from Uranus.

by the Voyager magnetometer team (R. P. Lepping, private communication, 1986). The dashed line is an estimate of the electron plasma frequency f_p described in detail in section 3.1. The upper panel of Figure 1 provides basic information on the location of Voyager 2 as a function of time, including radial distance R and magnetic latitude λ_m. The magnetic latitude is calculated on the basis of the OTD field model with no external contributions.

Figure 1 shows the concentration of plasma wave activity centered around the time of closest approach to the planet at about 1800 SCET (spacecraft event time). The most intense wave activity is the band observed almost continuously from 1200 through 2100 SCET at about one-third f_c. This emisson steps from one channel to the next over time, approximately following the f_c contour, but at a frequency of about $f_c/3$. This band consists of whistler mode waves in the form of chorus and hiss and is discussed by *Coroniti et al.* [this issue]. The sharp, intense spike near 1715 SCET at low frequencies is not plasma wave activity at all but is the response of the plasma wave receiver to micron-sized dust impacts on the spacecraft at the ring plane, discussed in detail by *Gurnett et al.* [this issue]. Dust impacts cause a broad spectrum, peaking at the lowest frequencies; hence it is straightforward to eliminate dust as the source of band-limited emissions which are the subject of this paper. The bursty emissions found occasionally just above the f_c contour from around 1230 through 2100 SCET are the Bernstein waves of interest in this paper. This paper will also briefly address the bursty emissions near 1920 SCET below f_c as possible electrostatic emissions.

2.1. *Bernstein Waves*

The plasma wave spectrum in Figure 1 is organized by the f_c contour. Waves just below the contour are generally whistler mode waves. Those just above the contour we classify as $(n + \frac{1}{2})f_c$ or Bernstein mode emissions. The wave activity in the three or four channels at the highest frequencies, especially with smoothly varying amplitudes, is radio emissions propagating at frequencies above the plasma frequency [*Gurnett et al.*, 1986]. Prior to closest approach (designated CA in Figure 1) there is a sizable gap in frequency between the bursty electrostatic waves and the more smoothly varying radio waves.

Subsequent to the closest approach there is no visible gap (to the resolution of the spectrum analyzer channel spacing) between the bursty electrostatic waves and the smoothly varying radio emissions. We rely, in part, on the bursty nature of electrostatic waves, as characterized at Earth [*Kurth et al.*, 1979], Jupiter [*Kurth et al.*, 1980], and Saturn [*Kurth et al.*, 1983] as a fairly reliable signature of electrostatic waves. The bursty character of Bernstein waves is expected as a consequence of the microscopic plasma instability and the accompanying localization and propagation effects [*Kurth et al.*, 1980].

The $(n + \frac{1}{2})f_c$ emissions are fairly well understood, theoretically, and the spectrum follows one of a fairly restricted range of possible forms. These have been classified at Earth by *Hubbard and Birmingham* [1978] and in a slightly different form by *Christiansen et al.* [1978]. The emissions are usually limited to frequencies above f_c and below the upper hybrid resonance (UHR) frequency

$$f_{\mathrm{UHR}} = (f_c^2 + f_p^2)^{1/2} \tag{1}$$

where $f_p[\mathrm{Hz}] = 9000(n_e[\mathrm{cm}^{-3}])^{1/2}$ is the electron plasma frequency and n_e is the electron density. The most intense band is usually the lowest band near $\frac{3}{2} f_c$ or the highest-frequency band—that which includes the upper hybrid resonance frequency [*Kurth et al.*, 1979]. The intermediate bands may or may not be present but will be at lower amplitudes than the $\frac{3}{2}$'s band. The amplitudes of the intermediate bands decrease with increasing harmonic number.

The above general guidelines help to interpret the spectrum shown in Figure 1. The most prominent Bernstein mode activity is centered at 1315 SCET with the most intense activity lying in the 1.00- and 1.78-kHz channels, well above f_c. Some very low level activity occurs between 1345 and 1500, with most of the emissions lying in the channel immediately above the f_c contour, indicating activity in the $\frac{3}{2}$'s band. Two brief but intense bursts occur at about 1600 SCET at 3.11 kHz and near 1705 SCET in the 10-kHz channel. An extended period of Bernstein activity begins at 1740 in the 10-kHz channel and moves into the 17.8-kHz channel at about 1750 SCET. We interpret the bursty emissions beginning at about 1900 SCET at 10 kHz and extending to 2045 SCET between 3.11 and 10 kHz as Bernstein waves as well, although there is possible confusion with the sporadic narrow-band electromagnetic emissions reported by *Kurth et al.* [1986] in this interval.

The burst of emission in the 3.11-kHz channel at 2130 SCET is thought to be a burst of sporadic narrow-band electromagnetic emissions as opposed to electrostatic emissions; however, it is really not possible to be sure in this case, because of uncertainties in the plasma frequency at this time. The bursty wave activity beginning at 1145 SCET in the 10- and 17.8-kHz channels and continuing until about 1430 SCET is thought to be electromagnetic radio wave activity as well, although the character of the emission is not smoothly varying like the radio emissions at 31.1 and 56.2 kHz during the same interval.

We return, now, for a detailed inspection of the electrostatic waves outlined above, beginning with the event centered around 1315 SCET. Figure 2 provides an expanded view of the time interval between 1215 and 1415 SCET for a limited frequency range. The amplitudes of the emissions in this event are in the range of 100 μV/m, similar to the amplitudes observed at Saturn [*Kurth et al.*, 1983] and the Earth [*Belmont et al.*, 1983]. Superimposed on Figure 2 is the f_c contour (solid line) and dashed lines representing harmonics of f_c.

As can be seen from Figure 2, the event has a duration of about 1 hour and covers the range from 562 Hz (just above the local electron cyclotron frequency) to 3.11 kHz. At 1315 SCET, where the cyclotron frequency is approximately 450 Hz, this frequency range suggests that bands up to the seventh harmonic of the cyclotron frequency are excited although the response at 3.11 kHz is most likely due to signals at a lower frequency but still within the wings of the 3.11-kHz filter response. In fact, for a signal lying between the fifth and sixth harmonics of f_c, one would expect nearly equal response in the 1.78- and 3.11-kHz channels. Because the 1.78-kHz response is considerably greater than that at 3.11 kHz, we suggest the emission responsible for the signal detected in the 1.78-kHz channel is due to a relatively intense band between $3f_c$ and $4f_c$.

On the basis of the expected behavior of the $(n + \frac{1}{2})f_c$ spectrum outlined above, it is most likely that the observed response is due to an intense band between $3f_c$ and $4f_c$, which implies that f_{UHR} also lies within this band ($f_{\mathrm{UHR}} \approx 1.6$ kHz). The response at 1.0 kHz, then, would be due primarily to the $\frac{5}{2}$'s band while the $\frac{3}{2}$'s emission appears in the 562-Hz channel. At 1250 SCET it seems that only the harmonic band including f_{UHR} is excited, either the $\frac{5}{2}$'s or $\frac{7}{2}$'s band in this case. Later, at 1340 SCET, it is again only the upper hybrid resonance band which is excited, probably between the third and fourth harmonics of the cyclotron frequency.

The location of the event at 1315 SCET is quite interesting. According to the plot of λ_m in Figure 1 and the listing of magnetic latitude given at the bottom of Figure 2, both derived from the OTD model, the event lies very close to the magnetic equator. It is a well-known characteristic of the $(n + \frac{1}{2})f_c$ emissions that they are found preferentially at the magnetic equator at Earth [*Belmont et al.*, 1983; *Canu et al.*, 1984], Jupiter [*Kurth et al.*, 1980], and Saturn [*Kurth et al.*, 1983]. *Barbosa* [1985] has provided a solid theoretical basis for the localization of the Bernstein emissions very close to the minimum $|\mathbf{B}|$ surface. The concentration of intense Bernstein emissions at the magnetic equator is such a reliable characteristic of the emission that we suggest the event in Figure 2 is remarkable because it is actually displaced from the OTD equator. The implications of this will be discussed below in section 3.2.

Returning now to Figure 1, the remaining events lying above f_c on the inbound leg appear to be $\frac{3}{2}$'s emissions because of their close proximity to the f_c contour. The events at 1600 and 1705 SCET are interesting because of their large amplitude but brief duration. The event at 1600 is nearly 1 mV/m and rivals the more intense events at Earth and Jupiter. The spacecraft is well off the magnetic equator at both times, so it is not clear why the waves appear in these particular locations. It should be noted, however, that intense upper hybrid events are known to occur at large ($\sim 50°$) magnetic latitudes at the Earth [*Kurth et al.*, 1979]. It is interesting that 1600 is approximately the time when Voyager 2 passed inside the minimum L shell for the moon Ariel [*Ness et al.*, 1986]. Perhaps the brief emission at 1600 is due to a disturbance on or near the minimum L shell of Ariel. There is no apparent satellite L shell crossing associated with the event at 1705 SCET.

Beginning at about 1740 a much more continuous set of emissions above f_c can be found which extends to 2045 SCET. These emissions are not as intense as those near 1315 SCET; however, the spacecraft remains well off the magnetic equator during the entire interval. The ~ 30-μV/m amplitudes observed between 3.11 kHz and 17.8 kHz are reminiscent of Bernstein mode amplitudes observed at Saturn [*Kurth et al.*,

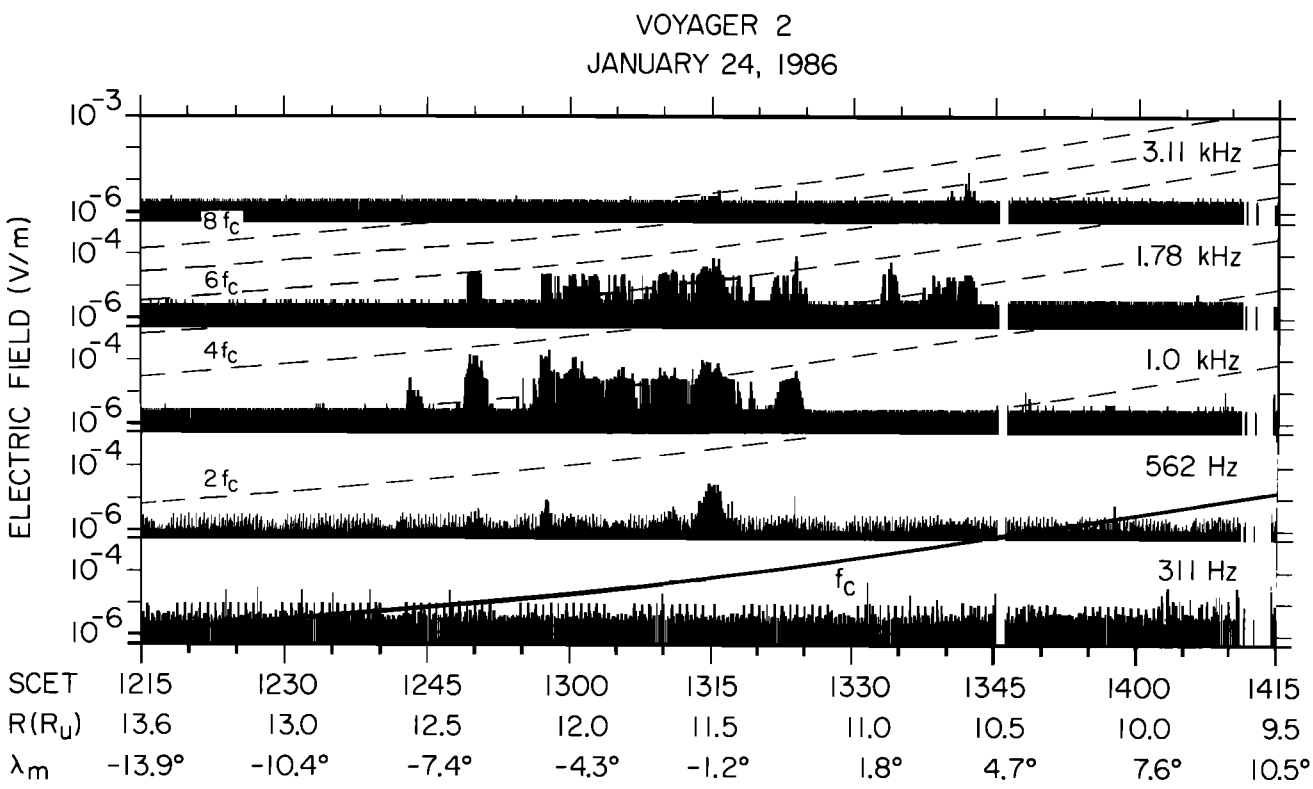

Fig. 2. A detailed plot of the plasma wave intensities observed near the magnetic equator based on the OTD model of *Ness et al.* [1986]. The primary emission is thought to be in the band between $3f_c$ and $4f_c$ near f_{UHR}. The apparent offset of the centroid of this event (1315 SCET) from the OTD equator suggests that the minimum |B| surface lies a degree or so south of the OTD equator.

1983]. It is unfortunate that Voyager 2 did not sample the magnetic equator at these small radial distances ($\lesssim 8\ R_U$), because our experience at the other planets with magnetospheres would lead us to expect the most intense Bernstein modes there. The weak emissions seen in Figure 1 are most likely indicative of the presence of the stronger waves at lower latitudes. Notice that the interval of 1740–2045 SCET corresponds to a local minimum in magnetic latitude according to Figure 1. In fact, this local minimum is accentuated in an improved field model known as Q_3, based on a spherical harmonic analysis; Voyager 2 actually came within about 5° of the Q_3 equator during this interval (M. Acuña, private communication, 1986).

The frequency of the bursty electrostatic waves between about 1740 and 1920 suggests that these are $\frac{3}{2}$'s bands near the upper hybrid resonance frequency. The presence of the smoothly varying radio emissions at just slightly higher frequencies in this interval suggests that the local plasma frequency cannot be very much higher than the observed frequency of the electrostatic waves since higher plasma densities would cut off the propagation of the radio waves. Beyond 1920 the bandwidth of the electrostatic wave activity expands to fill the gap between the radio emissions and f_c, implying the presence of emissions between each pair of f_c harmonics from f_c to f_{UHR}. At 2045 this implies that the highest-frequency emissions lie between $5f_c$ and $6f_c$.

It should be noted that an alternative identification exists for the wave activity between 1900 and 2045 SCET between the f_c contour and the smoothly varying radio emissions at 17.8 kHz. The signature of these emissions is similar to the bursty nature of the radio emission reported in the same frequency range but at larger distances by *Kurth et al.* [1986]. We prefer the identification of these waves as electrostatic emissions because of the high rate of occurrence compared to the electromagnetic waves previously reported and the fact that there is a very abrupt transition from the bursty character to the smoothly varying radio emissions both in the 17.8-kHz channel at 1900 SCET and in the 10-kHz channel at about 2050 SCET. This transition is just what would be expected as one leaves the electrostatic wave regime below f_p to the radio regime above f_p. The broadband cessation of wave activity near 2045 SCET is also suggestive of an electrostatic wave behavior since the flux of energetic electrons is dropping rather rapidly in this regime. The gradient in flux could easily result in a decrease in electrostatic wave activity; however, this gradient would have little to do with the propagation of radio waves through the region.

In order to give higher spectral and temporal resolution plasma wave information, a number of brief waveform observations were scheduled throughout the encounter. The waveform observations utilize a special high data rate mode of the plasma wave instrument in which the differential voltage across the antenna is sampled at a rate of 28.8 kHz, providing spectral information from about 40 Hz to 12 kHz. These waveform measurements compete with the imaging system as well as other instruments for tape recorder space and hence cannot occur very frequently. Fortunately, one of these observations occurred at about 1920 SCET; the data are presented in Plate 1.

Plate 1 is in the form of a frequency-time spectrogram in which the amplitudes of waves are plotted as a function of time (abscissa) and frequency (ordinate). The amplitude is rep-

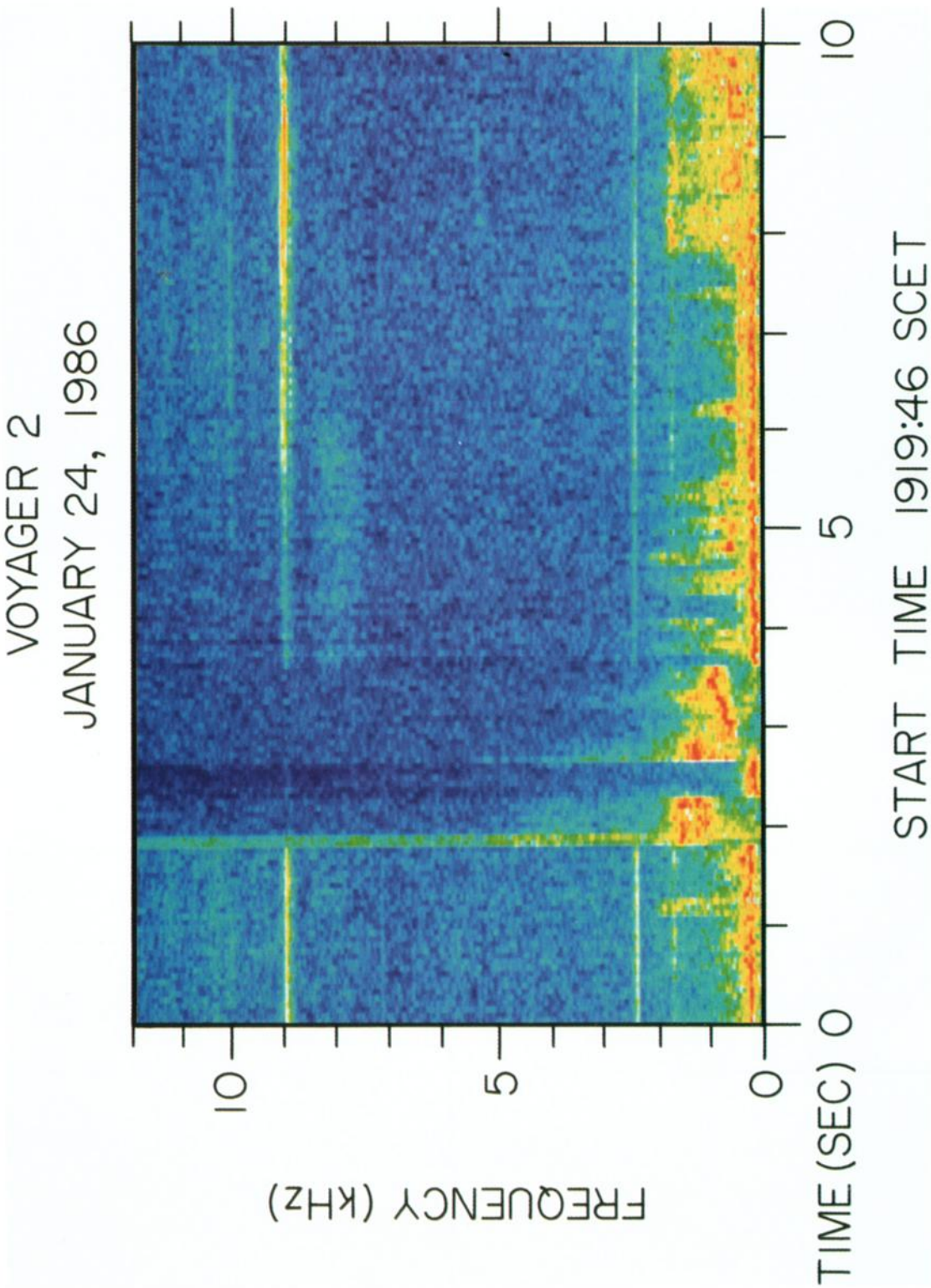

Plate 1. A frequency-time spectrogram obtained at about 1920 SCET near the outbound crossing of the Miranda L shell. The narrow-band emission at 9 kHz is the $\frac{3}{2}$'s emission, and the intense bursty emissions visible at lower frequency are emissions associated with this turbulent region. Some of these lower-frequency emissions may be electrostatic in nature; however, the modes have not been determined.

resented by a color scheme in which red is most intense and blue is least intense. The spectrogram has a time scale of 10 s. The signal of interest in Plate 1 is the narrow band at 9 kHz. The band does not appear to be continuous, indicating temporal variations in amplitude which would be consistent with the spiky appearance of the waves in Figure 1. However, there is an intense burst of low-frequency noise which occurs about 2 s into the frame in Plate 1 which captures the automatic gain control circuitry and reduces the gain of the receiver. Hence some or all of the observed intensity variation of the 9-kHz band may be instrumental in nature. The narrow band at 2.4 kHz is interference from the power supply and is present in virtually all of the Voyager waveform samples. The weaker, narrow tone at about 1.8 kHz appears less regularly, but often enough to be a likely interference effect, although the source is unknown.

The bandwidth of the 9-kHz emission is about 200 Hz or about 2% of the center frequency. This is an extremely narrow band emission. Typical bandwidths for the $\frac{3}{2}$'s emission at Saturn were about 25% [*Kurth et al.*, 1983]. We also note the presence of an even narrower (and less intense) band at about 10 kHz in Plate 1. (There are no known interference sources at 9 or 10 kHz; emission lines at these frequencies are very uncommon in the Voyager data set except in certain examples of narrow-band electromagnetic emissions at Jupiter [*Gurnett et al.*, 1983]. Hence we are confident these lines are not due to interference.) Since the cyclotron frequency at this time is about 5.4 kHz, the second band cannot be the $\frac{5}{2}$'s band but is probably an additional component to the spectrum of the $\frac{3}{2}$'s band. Observation of multiple lines within a single harmonic band are common at the Earth, and examples can be found in the Hawkeye, IMP 6, and ISEE data sets. *Koons and Fennell* [1984] have reported complex band structures for terrestrial $(n + \frac{1}{2})f_c$ emissions as observed from the SCATHA satellite. The most complete theoretical discussion of the generation of fine structure in electron cyclotron harmonic emissions is given by *Horne et al.* [1987] in which three different mechanisms are discussed, dealing with multiple features in the distribution function or dispersion curves which result in growth at different frequencies.

2.2. *Other Possible Electrostatic Modes*

Until now, we have only considered Bernstein mode waves. These modes are relatively simple to identify in the plasma wave spectrum because of their location between f_c and f_{UHR}. Also, we have discussed the intense band of electromagnetic whistler mode noise at about one-third the electron cyclotron frequency which dominates the spectrum below f_c. For the most part there are few other candidates for electrostatic waves in the Uranian magnetosphere. One exception, however, is the brief interval around 1920 SCET. At this time there is a dramatic decrease in the amplitude of the whistler mode band and the appearance of a number of very intense, bursty emissions covering the frequency range from 10 Hz to the electron cyclotron frequency near 5.5 kHz.

The region near 1920 SCET corresponds to the outbound crossing of the instantaneous location of the Miranda L shell and also coincides closely with the "plasma edge" [*Bridge et al.*, 1986] which the plasma science investigators suggest may be related to the convection limit. In any case, the plasma wave spectrum is highly turbulent and complex. The intense band of whistler mode activity appears to subside dramatically in the region near 1920 in favor of more sporadic types of emissions. As suggested by *Kurth et al.* [1986], a number of different types of wave modes may exist in this region, including whistler mode waves in the frequency range of 500 Hz to 2 kHz and perhaps Doppler-shifted ion acoustic waves below a few hundred hertz. The waveform frame shown in Plate 1 is from this same interval and shows evidence of very bursty emissions near 1 kHz. Since this is in the realm of whistler mode emissions, however, it is very difficult to guess at the electrostatic versus electromagnetic nature of the waves found in this region. The very bursty character suggests that these and other very low frequency emissions in this complex region may be electrostatic in nature. Unfortunately, there is insufficient information with which to identify the various modes.

3. IMPLICATIONS OF THE ELECTROSTATIC WAVE OBSERVATIONS

The various wave emissions having been thus identified, it is possible to make several inferences on the Uranian magnetosphere based on previous experience with electrostatic waves at other planets.

3.1. *Electron Density*

The detection of the Bernstein mode electrostatic waves in the magnetosphere of Uranus provides some information on the electron density at a number of locations. Using our identification of upper hybrid emissions and the fairly well understood constraints on the spectral range of emissions based on critical frequencies of the plasma, we can use the electrostatic waves along with some clues provided by the cutoff of radio emissions at higher frequencies to specify the electron density at several points along the Voyager 2 trajectory. The dashed line in Figure 1 represents a plasma frequency profile based on the arguments to follow. The solid circles along this profile are locations where there is significant information in the radio and plasma wave spectrum, and the dashed line is a simple curve connecting the circles; there is little information to suggest any further detail.

The identification of the cyclotron harmonic band including the upper hybrid resonance frequency leads to an estimate of the electron density since f_{UHR} is a function of f_c, which is well known from the magnetometer measurements, and f_p. The discussion of Figure 2 in section 2.1 concluded that the emission near 1315 SCET was largely due to emissions in the second and third harmonic bands, with only weak emission in the first band. Since the most intense emission in a set of $(n + \frac{1}{2})f_c$ emissions is either the $\frac{3}{2}$'s band or the upper hybrid band, we conclude that the emission in the third harmonic band is the upper hybrid band at about 1.6 kHz. The corresponding electron plasma frequency is then very close to 1.6 kHz, and the density is approximately 0.03 cm^{-3}. The uncertainty in this estimate is due to the coarse frequency spacing of the spectrum analyzer channels. If we use half the channel spacing between the 1- and 1.78-kHz channels as the uncertainty in the upper hybrid resonance frequency, the electron density has an uncertainty of about 50%.

For completeness it should be noted that because the Bernstein bands are separated by approximately the cyclotron frequency, there is a possible difference between the frequency of the upper hybrid band and the actual upper hybrid resonance frequency of up to f_c. For the event at 1315, f_c is about equal to half the spectrum analyzer channel spacing; hence the uncertainty due to the difference between the frequency of the

upper hybrid band and f_{UHR} is very close to the uncertainty quoted above.

The profile through the event at 1315 SCET is continued to the left in Figure 1 toward the magnetopause and connected to points near 1100 and 1150 SCET at about 1.2 kHz. These points are inferred from the low-frequency cutoff of very weak continuum radiation detected in waveform samples obtained at those times.

It is possible that the brief spikes at 1600 and 1705 SCET occur at $3f_c/2 \approx f_{UHR}$, in which case the respective electron densities are about 0.1 cm^{-3} and 1 cm^{-3}, respectively. However, since only the $\frac{3}{2}$'s emission is present, the upper hybrid frequency could be at much higher frequencies, and the upper hybrid band is simply not excited. In view of the cold ion density of about 0.5 cm^{-3} reported by *McNutt et al.* [1987] near 1700 SCET, however, we doubt that f_{UHR} is much larger than f_c; hence we suggest the quoted densities are valid. The uncertainties at 1705 would imply no disagreement between the McNutt et al. density and that derived from the Bernstein emission.

No profile for f_p is drawn from about 1400 to 1715 SCET since there is very little information in the plasma wave spectrum to do so. Because the whistler mode has an upper frequency cutoff that is less than the lower of f_p and f_c, we could say that the upper frequency extent of the whister mode emissions is a lower limit for f_p in the interval. However, as pointed out by *Coroniti et al.* [1984], there is often a sizable gap between the upper frequency limit of the whistler mode emissions and the cyclotron frequency and hence it is likely that such a profile would be an underestimate of f_p.

The electron density information provided in the interval 1740–2045 SCET is obviously dependent on the conclusion that the waves above f_c and below the smoothly varying radio emissions are all of the Bernstein variety and not sporadic electromagnetic emissions. Should this assumption be incorrect, then little can be said at all about electron densities in this time interval on the basis of the plasma wave spectrum. Let us proceed, however, on the basis that our identification of these waves is correct. We shall return to this question after suggesting a feasible plasma density profile.

The plasma frequency profile during the outbound leg of the trajectory is based primarily on the transition from a bursty electrostatic wave spectrum to the smoothly varying radio wave spectrum. Two key points occur at about 1900 SCET in the 17.8-kHz channel and at about 2050 SCET in the 10-kHz channel. If one assumes the plasma density is decreasing with time through this region, then the transition from the electrostatic spectrum to the electromagnetic spectrum implies a propagation cutoff. In detail, the cutoff occurs at either the $R = 0$ cutoff [*Stix*, 1962] if the radio waves are propagating in the extraordinary mode or at f_p if they are ordinary mode emission. *Warwick et al.* [1986] identified the radio emission at higher frequencies as being in the extraordinary mode, so we assume the cutoff is at $f_{R=0}$. Given that

$$f_{R=0} = f_c/2 + [(f_c/2)^2 + f_p^2]^{1/2} \quad (2)$$

we can calculate f_p at 1900 and 2050 SCET assuming the $f_{R=0}$ is at the center frequency of the respective channels at each cutoff. Therefore at 1900 SCET, $f_{R=0} = 17.8$ kHz, and hence $f_p = 13.7$ kHz and $n_e = 2.3$ cm^{-3}. Similarly, for 2050 SCET where $f_{R=0} = 10$ kHz, $f_p = 9.1$ kHz and $n_e = 1$ cm^{-3}.

Using the upper frequency extent of the Bernstein mode emissions as a guide, another possible signature of a density cutoff occurs at about 1820 SCET, where there is a local minimum in the intensity of radio emissions at 31.1 kHz. We can assume the upper limit of $f_{R=0}$ is near the center frequency of the 31.1-kHz channel and can calculate $f_p = 25.3$ kHz or $n_e = 7.8$ cm^{-3}. A lower limit would be to assume $f_{R=0}$ is a half channel spacing lower than 31.1 kHz. In this case, $f_p = 17.7$ kHz or $n_e = 3.8$ cm^{-3}. Prior to 1800 the Bernstein waves are limited to the 10-kHz channel; hence we assume that the plasma frequency is in the same frequency range, and hence n_e is likely to be near 1 cm^{-3} between 1740 and 1800 SCET.

The plasma frequency profile we have developed for the interval from 1740 to 2050 SCET, then, starts near 10 kHz at the beginning of the interval, climbs to the range of 18–25 kHz for a peak at about 1820, falls to about 14 kHz by 1900 SCET, and finally drops to 9 kHz at 2050 SCET. There is no basis in the plasma wave spectrum to connect these points with anything other than a smooth curve; however, it is very likely that real deviations from this profile could exist.

A comparison of this profile is generally consistent with the cold ion densities given by *McNutt et al.* [1987]; the hot ion densities are about an order of magnitude smaller and hence are negligible to the uncertainties in the plasma wave derivation. Near 1800 the plasma measurements yield a cold density of about 0.5 cm^{-3}. A local peak is found near 1820 SCET, but with a value of only about 2 cm^{-3}, to be compard with the plasma wave estimate between about 4 and 8 cm^{-3}. At 1900 the plasma science density determination is approximately 2.5 cm^{-3}, to be compared to 2.3 cm^{-3} by our analysis. At 1938 SCET the plasma investigation [*McNutt et al.*, 1986] reports a dramatic charging event which brought the spacecraft potential to as much as 400 V negative. The charging interval was over somewhat before 2200 SCET. During the charging event, McNutt et al. reported tentative densities of 0.3–1 cm^{-3}, well within agreement with the plasma wave estimate of 1 cm^{-3} at 2050 SCET, especially in view of any difficulties the charging might cause the density determination by the plasma instrument.

One other point is highlighted in Figure 1 at about 2012 SCET and 9.6 kHz. This point has been derived by *Coroniti et al.* [this issue] on the basis of an analysis of the very intense whistler mode emissions at 562 Hz. To explain the spectrum of the whister mode emission, it is necesary to have a density of about 1.14 cm^{-3} at 2012 SCET.

The plasma investigation's density profile is more complex than that described above from the plasma wave spectrum. For example, *McNutt et al.* [1987] show local minima in the density profile at 1810 and 1840 SCET of about 0.5–1 cm^{-3} which are not suggested by the Bernstein wave spectrum. It is doubtful that the plasma wave spectrum is deterministic enough to actually be in disagreement with this aspect of the plasma investigation's profile, however, and we could not express any strong disagreement with the plasma team's determination. The only specific disagreement of any magnitude is the peak at 1820 SCET, which the plasma wave spectrum suggests is between 4 and 8 cm^{-3}, compared to about 2 cm^{-3} according to the plasma instrument. The local minimum in the radio emission amplitude which is the primary basis of the plasma wave determination could possibly be due to a temporal variation or a remote refraction effect. In summary, we believe the results deduced above are in general agreement with the densities determined by the plasma team.

In view of the consistency of the density profile with the density determined by plasma observations, it seems more

likely that our interpretation of the sporadic emissions between 1900 and 2045 SCET as Bernstein waves is correct and the emissions are not the electromagnetic waves reported by *Kurth et al.* [1986]. Even if the density is as low as 0.3 cm^{-3}, as reported by *McNutt et al.* [1987] in the charging region, only the emissions in the 10-kHz channel could propagate freely, above the plasma frequency.

The identification of the mode of the radio emissions in the range of 10–56 kHz is highly dependent on the presumed source location for the emission; hence the extraordinary mode identification is quite uncertain (M. L. Kaiser, private communication, 1986). We argue, however, that between 1700 and 1900 SCET, when the cyclotron frequency is quite large, an identification of the radio wave mode as being ordinary would significantly raise the f_p profile and the consistency with the plasma science density determinations would be lost. Owing to the circular nature of this line of reasoning, there is little chance that a definite determination of the radio wave mode can be reached. We suggest, however, that the extraordinary mode interpretation used herein seems to yield the most consistent profile for f_p.

3.2. *Location of the Magnetic Equator*

As described in section 2.1, the $(n + \frac{1}{2})f_c$ waves near 1315 SCET are obviously clustered around the magnetic equator. This is a well-established characteristic of the emissions at the other planets and therefore is not surprising at Uranus. A reasonable explanation for the equatorial confinement is that the combined effects of propagation and amplification of electrostatic Bernstein waves single out the magnetic equator (minimum |B| surface) as a preferential location for the generation of the noise [*Barbosa*, 1985]. Since Bernstein waves at the Earth, Jupiter, and Saturn also exhibit the equatorial confinement, we must conclude that very general processes are at work. While the event in Figure 2 obviously straddles the magnetic equator by about ±4°, it seems to be offset to negative magnetic latitudes. We suggest this is evidence that the latitude scale in Figure 2 (based on the OTD model) is not valid at this radial distance.

Before proceeding, it is necessary to establish the actual deviation of the Bernstein waves from the OTD equator. If one simply takes the midpoint of the wave activity which begins at about 1245 and ends near 1345, it seems that 1315 SCET is a good centroid for the event. Further, the maximum bandwidth and perhaps amplitude is achieved at 1315 as well. We use these two different lines of reasoning to suggest that the center of the event is at 1315 SCET and the deviation from 0° magnetic latitude is significant. On the basis of a weighted average of wave intensities, it would appear that selecting a time even earlier, and hence further south, would be reasonable.

Actually, it would not be surprising that the OTD model does not predict an accurate position for the magnetic equator at a distance of 11.5 R_U. *Ness et al.* [1986] showed very clearly that the model begins to deviate from the data at about this distance. While it may be possible that the electrostatic waves are actually displaced from the magnetic equator, we suggest that there is no obvious mechanism to displace the waves. We believe, instead, that the centroid of the electrostatic wave emission is perhaps the best locator of the magnetic equator (minimum |B| surface) that is available through the Voyager measurements. As a result, we believe the actual equator is at least 1° further south than predicted by the OTD model.

Perhaps, a more refined field model would correct the offset. It is unlikely, though, that taking higher moments into account would be useful, since the higher moments generally affect the measurements at much closer distances. We suggest it is much more likely that a model which incorporates a ring current in a broad range of distances around 10 R_U might be more reasonable. Another possibility is that currents flowing on the magnetopause might result in minor warping of the shape of the outer magnetosphere. We do not propose to generate a new field model, but we do suggest that future modeling efforts attempt to match the location of the Voyager 2 inbound magnetic equator crossing to the centroid of the Bernstein wave event at 1315 SCET.

3.3. *Superthermal Electron Flux*

It is possible to make some inferences on the flux of electrons which presumably are responsible for the Bernstein mode event in Figure 2. We employ the "critical flux" concept of *Barbosa and Kurth* [1980] appropriately scaled to Uranus. In this theory, linear analysis of the spatial amplification of the $\frac{3}{2} f_c$ band emission in a dipole magnetic field is used to calculate a flux level of anisotropic ($E_\perp > E_\parallel$) electrons that can yield 10 e foldings of wave amplitude. Equation (26) of *Barbosa and Kurth* [1980] is modified to

$$Tj_\perp{}^* = 5.4 \times 10^4 \left(\frac{T/T_c}{4}\right)^2 \left(\frac{T_c}{30\ \text{eV}}\right) \quad \text{cm}^{-2}\ \text{s}^{-1}\ \text{sr}^{-1} \qquad (3)$$

with $B_U = 0.23$ G, $R_U = 25{,}600$ km, $n_e = 3.9 \times 10^{-2}$ cm^{-3}, $R = 11.5$, $\overline{\delta\omega} = 0.1$, and $\omega = 1.5$. A value of $T_e = 10$–30 eV for the background electron temperature is derived from the plasma science experiment results obtained closer to Uranus [*Bridge et al.*, 1986; *McNutt et al.*, 1987], while the density is based on the identified UHR emission in Figure 1. The ±4° confinement near the magnetic equator reported above suggests that the noise is being driven by superthermal electrons with velocities 2–3 times the thermal speed of the background gas [*Barbosa*, 1985]. Hence the superthermals have energies 4–9 times the 10- to 30-eV background electrons or are of the order of a few hundred electron volts.

The measured flux of electrons at this time is $\sim 3 \times 10^{-5}$ cm^{-2} s^{-1} [*Bridge et al.*, 1986]. To compare with (3), some assumption about the effective solid angle over which the electrons are dispersed is needed. A factor of 2π times the result in (3) yields 3×10^5 cm^{-2} s^{-1}, and this compares well with the observed value. This agreement indicates that the conditions for sufficient growth of the waves are present and also demonstrates the overall consistency of the theory between different planets.

4. SUMMARY

We have shown evidence of Bernstein mode electrostatic waves in the magnetosphere of Uranus that are similar in most respects to those observed at Earth, Jupiter, and Saturn. The intensities are comparable to those at Earth and Saturn, but somewhat weaker than Jovian Bernstein waves. Since Voyager 2 did not traverse the magnetic equator within about 8 R_U, it is possible that more intense waves exist in the inner region of the magnetosphere near the magnetic equator. The most intense waves were measured at the magnetic equator, but at a distance of about 11.5 R_U. The Bernstein waves are resonant with electrons of a few hundred electron volts, and

the measured fluxes are similar to a calculation of the critical flux required to drive the instability.

The location of the centroid of the event near 1315 SCET probably marks the location of the actual magnetic equator, and the slight displacement from the OTD magnetic equator is probably due to the deviation of the model from the actual field at large distances and the lack of external field sources in the model.

Electron densities derived from an analysis of the plasma wave and radio spectrum in general and the Bernstein waves in particular lead to a profile that is consistent with measurements by the plasma science instrument. Further, the consistency with the plasma measurements implies that radio emissions in the frequency range of 10–17.8 kHz observed shortly after closest approach are propagating in the extraordinary mode.

Note added in proof. A recent study of the plasma science investigation's electron observations [*Sittler et al.*, this issue] states that "electron fluxes remained close to the instrument detection threshold" in the interval near the magnetic equator crossing on the dayside. The relationship of this result to the fluxes reported by *Bridge et al.* [1986] is unclear; the use of $T_e = 10$–30 eV in section 3.3 should probably be regarded with some caution. Nevertheless, it would be very difficult to explain the Bernstein wave spectrum at the magnetic equator (1315 SCET) with a plasma density of much less than about 0.02 cm^{-3}.

Acknowledgments. We thank R. P. Lepping, J. E. P. Connerney, and M. H. Acuña of the Voyager Magnetometer Team and M. L. Kaiser of the Voyager Planetary Radio Astronomy Team for several useful discussions as well as for access to their respective data sets. The research at the University of Iowa was supported by the National Aeronautics and Space Administration through contracts 954013 and 957723 with the Jet Propulsion Laboratory. The research at TRW was supported by NASA through contract 954012 with the Jet Propulsion Laboratory. The research at UCLA was supported by the National Science Foundation through grant ATM 86-06857.

The Editor thanks R. B. Horne and J. L. Roeder for their assistance in evaluating this paper.

REFERENCES

Ashour-Abdalla, M., and C. F. Kennel, Nonconvective and convective electron cyclotron harmonic instabilities, *J. Geophys. Res.*, *83*, 1531, 1978.

Barbosa, D. D., Electrostatic wave propagation and trapping near the magnetic equator, *Ann. Geophys. Gauthier Villars*, *3*, 63, 1985.

Barbosa, D. D., and W. S. Kurth, Superthermal electrons and Bernstein waves in Jupiter's inner magnetosphere, *J. Geophys. Res.*, *85*, 6729, 1980.

Belmont, G., D. Fontaine, and P. Canu, Are equatorial electron cyclotron waves responsible for diffuse auroral electron precipitation?, *J. Geophys. Res.*, *88*, 9163, 1983.

Bridge, H. S., et al., Plasma observations near Uranus: Initial results from Voyager 2, *Science*, *233*, 89, 1986.

Canu, P., G. Belmont, and D. Fontaine, Role of the equatorial ECH waves in the generation of diffuse auroras: Contribution of the GEOS IMS spacecraft, Proceedings of the Conference on Achievements of the IMS, *Eur. Space Agency Spec. Publ., ESA SP-217*, 581, 1984.

Christiansen, P. J., M. P. Gough, G. Martelli, J. J. Bloch, N. Cornilleau, J. Etcheto, R. Gendrin, C. Beghin, P. Decreau, and D. Jones, GEOS-1 observations of electrostatic waves, and their relationship with plasma parameters, *Space Sci. Rev.*, *22*, 383, 1978.

Coroniti, F. V., F. L. Scarf, C. F. Kennel, and W. S. Kurth, Analysis of chorus emissions at Jupiter, *J. Geophys. Res.*, *89*, 3801, 1984.

Coroniti, F. V., W. S. Kurth, F. L. Scarf, S. M. Krimigis, C. F. Kennel, and D. A. Gurnett, Whistler mode emissions in the Uranian radiation belts, *J. Geophys. Res.*, this issue.

Gurnett, D. A., W. S. Kurth, and F. L. Scarf, Narrowband electromagnetic emissions from Jupiter's magnetosphere, *Nature*, *302*, 385, 1983.

Gurnett, D. A., W. S. Kurth, F. L. Scarf, and R. L. Poynter, First plasma wave observations at Uranus, *Science*, *233*, 106, 1986.

Gurnett, D. A., W. S. Kurth, F. L. Scarf, J. A. Burns, J. N. Cuzzi, and E. Grün, Micron-sized particle impacts detected near Uranus by the Voyager 2 plasma wave instrument, *J. Geophys. Res.*, this issue.

Horne, R. B., P. J. Christiansen, and M. P. Gough, Weak electrostatic waves near the upper hybrid frequency: A comparison between theory and experiment, *J. Geophys. Res.*, *92*, 3243, 1987.

Hubbard, R. F., and T. J. Birmingham, Electrostatic emissions between electron gyroharmonics in the outer magnetosphere, *J. Geophys. Res.*, *83*, 4837, 1978.

Kennel, C. F., and M. Ashour-Abdalla, Electrostatic waves and the strong diffusion of magnetospheric electrons, in *Magnetospheric Plasma Physics*, edited by A. Nishida, p. 245, Center for Academic Publications Japan, Tokyo, 1982.

Kennel, C. F., F. L. Scarf, R. W. Fredricks, J. H. McGehee, and F. V. Coroniti, VLF electric field observations in the magnetosphere, *J. Geophys. Res.*, *75*, 6136, 1970.

Koons, H. C., and J. F. Fennell, Fine structure in electrostatic emission bands between electron gyrofrequency harmonics, *J. Geophys. Res.*, *89*, 3015, 1984.

Kurth, W. S., J. D. Craven, L. A. Frank, and D. A. Gurnett, Intense electrostatic waves near the upper hybrid resonance frequency, *J. Geophys. Res.*, *84*, 4145, 1979.

Kurth, W. S., D. D. Barbosa, D. A. Gurnett, and F. L. Scarf, Electrostatic waves in the Jovian magnetosphere, *Geophys. Res. Lett.*, *7*, 57, 1980.

Kurth, W. S., F. L. Scarf, D. A. Gurnett, and D. D. Barbosa, A survey of electrostatic waves in Saturn's magnetosphere, *J. Geophys. Res.*, *88*, 8959, 1983.

Kurth, W. S., D. A. Gurnett, and F. L. Scarf, Sporadic narrow-band radio emissions from Uranus, *J. Geophys. Res.*, *91*, 11,958, 1986.

McNutt, R. L., Jr., et al., The low energy plasma in the Uranian magnetosphere, *Adv. Space Res.*, in press, 1986.

McNutt, R. L., Jr., R. S. Selesnick, and J. D. Richardson, Low-energy plasma observations in the magnetosphere of Uranus, *J. Geophys. Res.*, *92*, 4399, 1987.

Ness, N. F., M. H. Acuña, K. W. Behannon, L. F. Burlaga, J. E. P. Connerney, R. P. Lepping, and F. M. Neubauer, Magnetic fields at Uranus, *Science*, *233*, 85, 1986.

Scarf, F. L., and D. A. Gurnett, A plasma wave investigation for the Voyager mission, *Space Sci. Rev.*, *21*, 289, 1977.

Scarf, F. L., D. A. Gurnett, W. S. Kurth, F. V. Coroniti, C. F. Kennel, and R. L. Poynter, Plasma wave measurements in the magnetosphere of Uranus, *J. Geophys. Res.*, this issue.

Sittler, E. C., Jr., K. W. Ogilvie, and R. Selesnick, Survey of electrons in the Uranian magnetosphere: Voyager 2 observations, *J. Geophys. Res.*, this issue.

Stix, T. H., *The Theory of Plasma Waves*, p. 13, McGraw-Hill, New York, 1962.

Warwick, J. W., et al., Voyager 2 radio observations of Uranus, *Science*, *233*, 102, 1986.

D. D. Barbosa, Institute of Geophysics and Planetary Physics, University of California, Los Angeles, CA 90028.

D. A. Gurnett and W. S. Kurth, Department of Physics and Astronomy, University of Iowa, Iowa City, IA 52242.

F. L. Scarf, TRW Space and Technology Group, One Space Park, Redondo Beach, CA 90278.

(Received January 27, 1987;
revised April 21, 1987;
accepted April 27, 1987.)